

Investigating non-Gaussianity in Cosmic Microwave Background Temperature Maps using Spherical Harmonic Phases

Sarvesh Kumar Yadav^{1*}, and Rajib Saha^{1†}

¹Department of Physics, Indian Institute of Science Education and Research, Bhopal, 462066, India

Abstract

In the era of precision cosmology accurate estimation of cosmological parameters is based upon the implicit assumption of Gaussian nature of Cosmic Microwave Background (CMB) radiation. Therefore, an important scientific question to ask is whether the observed CMB map is consistent with Gaussian prediction. In this work we devise a new method where we use Rao's statistic based on sample arc-lengths to examine the validity of the hypothesis that the temperature field of the CMB is consistent with a Gaussian random field, by comprehensively testing correlations within a given ℓ mode and between nearby ℓ modes phases. This circular statistic is ordered and non-parametric. We performed our analysis on the scales limited by spherical harmonic modes ≤ 128 , to restrict ourselves to signal dominated region. To find the correlated sets of phases, we calculate the statistic for the data and 10000 Monte Carlo simulated random sets of phases and used 0.01 and 0.05 α levels to distinguish between statistically significant and highly significant detections. We apply our method on Planck satellite mission's final released CMB temperature anisotropy maps-COMMANDER, SMICA, NILC, and SEVEM along with WMAP 9 year released ILC map. We report that phases corresponding to some of the modes are non-uniform in these maps. We also report that most of the mode pairs are uncorrelated in each map, but a few are found to be correlated, which are different pairs in different maps. The detection of non-uniformity and correlations in the phases indicates presence of non Gaussian signals in the foreground minimized CMB maps.

*email:sarveshk@iiserb.ac.in

†email:rajib@iiserb.ac.in

Keywords: CMB anomalies, CMB Phase analysis, CMB non-gaussianity

1 Introduction

One of the central ideas in many cosmological models is that galaxies and large-scale structures in the universe have grown from small initial perturbations via a process of gravitational instability. In one of the most successful of such models, the primordial perturbations that seeded the initial gravitational instability were generated during a period of rapid expansion, known as inflation [1, 2]. The perturbations produced by inflation are said to be a statistically homogeneous Gaussian random field [3]. It is believed that the imprint of such perturbations are on the last scattering surface (LSS) of cosmic microwave background (CMB) at large angular scales. The statistical properties of the fluctuations on the LSS will be highly correlated to the primordial perturbation, making it a very useful probe for testing the Gaussianity of the primordial universe. Test of gaussianity becomes essential from the fact that the temperature and polarization power spectrum used to derive the cosmological parameters, assume that the statistical properties of the primordial CMB signal is gaussian. Their detection and identification allows to distinguish various inflationary models [4] making the investigation further relevant.

Unlike gaussianity, non-gaussianity can be of many types, making it difficult to quantify. As detection of non-gaussianity has far-reaching consequences for our understanding of the primordial universe [5], and hence one needs to test it with various statistical measures, each sensitive to distinct forms of the non-gaussianity present in CMB data. Though detected non-gaussianity might not have a primordial origin, they can lead us to better understand the foreground residuals and systematics present in the cleaned CMB maps.

Numerous studies on non-gaussianity for CMB missions such as COBE, MAXIMA, BOOMERanG, WMAP and Planck has been done. Many of these works are based on measures such as bispectrum [4, 6–12], trispectrum [13–16], skewness and kurtosis [17–20], spherical Mexican hat wavelet [21–33], minkowski functionals [34–38], directional spherical real morlet wavelet analysis [27], scaling index method [39, 40], method based on the N-point probability distribution function [41], skeleton statistics [42, 43], spectral distortions [44], neural-network [45], multipole vector [46], genus shift parameters [47, 48], bipolar spherical harmonics [49]. In many of these studies, the estimator is based on some phenomenological model and is capable of de-

testing certain types of non-gaussianity. Another way to check gaussianity is based on a blind test, one which is motivated by statistics rather than phenomenology; this has been done in some of the above-mentioned works. Most of the above-cited works use $a_{\ell m}$ or estimators derived using them. However not many studies using phases corresponding to the complex quantity $a_{\ell m}$, which will have a circular uniform random distribution, given $a_{\ell m}$ have gaussian distribution, have been undertaken. Some of such studies are using Kuiper statistics [50–52], temperature-weighted extrema correlation functions [53], using phase mapping technique [54–56], trigonometric moments of phases and Pearson’s random walks [57, 58]. The phases are related to the spherical harmonic coefficients $a_{\ell m}$ in a nonlinear way and are therefore sensitive to mode correlations of CMB in a different way. Some of the works mentioned above have reported the detection of non-gaussianity, and others had not detected any significant signal.

In the present article, we perform a model-independent study to investigate non-gaussianity in the Planck satellite mission’s final released cleaned CMB full-sky temperature anisotropy maps - COMMANDER, SMICA, NILC, SEVEM along with the final release of WMAP internal linear combination map. We use a new circular statistic known as the Rao’s spacing test [59], which is sensitive to multi-mode type non-uniformities in data phases (hence non-gaussianities in corresponding $a_{\ell m}$). This feature of non-uniformity has not been investigated in the literature earlier. We perform three distinct tests to investigate uniformity in phases of each ℓ mode and two other tests to examine correlations between a given ℓ mode and nearby ℓ modes.

We organize our paper as follows. In Section 2 we illustrate the basic formalism of this work by first describing the phases derived from the spherical harmonic coefficients and then presenting the details of the statistics used in the current work. In Section 3, we elaborate on the methodology applied on the data to detect the statistically significant signal. In Section 4, we present the results. Finally, in Section 5, we discuss and conclude.

2 Formalism

2.1 Spherical Harmonics Phases and Inflation

CMB fluctuations, over the last scattering surface can be mathematically expressed as,

$$\Delta(\theta, \phi) = \frac{(T(\theta, \phi) - \bar{T})}{\bar{T}} = \sum_{\ell=1}^{\infty} \sum_{m=-\ell}^{\ell} a_{\ell m} Y_{\ell m}(\theta, \phi), \quad (1)$$

where \bar{T} is the mean temperature over the whole sky, $T(\theta, \phi)$ is the temperature in the direction (θ, ϕ) on the celestial sphere in some coordinate system. The $Y_{\ell m}(\theta, \phi)$ are spherical harmonic functions, defined in terms of the Legendre polynomials $P_{\ell m}$ as,

$$Y_{\ell m}(\theta, \phi) = (-1)^m \sqrt{\frac{(2\ell + 1)(\ell - m)!}{4\pi(\ell + m)!}} P_{\ell m}(\cos\theta) \exp(im\phi), \quad (2)$$

where we have used the Condon-Shortley phase convention. In equation (1), the $a_{\ell, m}$ are complex coefficients and so one can write it as,

$$a_{\ell m} = |a_{\ell m}| \exp[i\psi_{\ell m}], \quad (3)$$

where $\psi_{\ell m}$ is the phase angle. If $\mathcal{R}(a_{\ell m})$ and $\mathcal{I}(a_{\ell m})$ represents real and imaginary parts respectively of the complex $a_{\ell m}$ then $\Psi_{\ell m}$ is written as,

$$\psi_{\ell m} = \frac{\mathcal{I}(a_{\ell m})}{\mathcal{R}(a_{\ell m})}. \quad (4)$$

As Δ is a real quantity, $\mathcal{R}(a_{\ell m}) = -\mathcal{R}(a_{\ell - m})$ and $\mathcal{I}(a_{\ell m}) = \mathcal{I}(a_{\ell - m})$ for odd m , $\mathcal{R}(a_{\ell m}) = \mathcal{R}(a_{\ell - m})$ and $\mathcal{I}(a_{\ell m}) = -\mathcal{I}(a_{\ell - m})$ for even m and $\mathcal{I}(a_{\ell m}) = 0$, for $m=0$. This implies that we have only ℓ numbers of independent phases corresponding to a given mode ℓ .

If the CMB temperature anisotropies constitute a Gaussian Random Field, the real and imaginary part of the $a_{\ell m}$ are both Gaussian distributed or equivalently, the $|a_{\ell m}|$ are Rayleigh distributed and phases $\psi_{\ell m}$ are uniformly random in $[0, 2\pi]$. The hypothesis that phases corresponding to gaussian $a_{\ell m}$ are uniform is known as the random phase hypothesis.

2.2 Rao's Spacing Test

In the current study, we use Rao's [60] statistics to test the random phase hypothesis of the CMB temperature maps. It is a powerful statistic for testing uniformity of circular data. In particular, it is more powerful than the popular Rayleigh Test and Kuiper's Test [61] when the underlying circular distribution is multimodal. Most of the earlier studies on the testing of non-uniformity of CMB phases are based on Kuiper's [61] V statistics. Unlike Kuiper's statistics which is based on empirical distribution function, Rao's statistics is goodness-of-fits test based on the idea that if the underlying circular distribution is uniform, successive observations should be approximately evenly spaced, about $2\pi/n$ apart, where n is the number of circular samples. Large deviations from this distribution, resulting from unusually large spaces or unusually short spaces between observations, signify

directionality. Further, it is invariant under a choice of the origin and is non-parametric ordered statistics applicable to circular data. Suppose we have a set of n circular variables $\{\theta_i\}$, $i = 1, \dots, n$ in the interval $[0, 2\pi]$ which are arranged in ascending order w.r.t a given zero direction and the sense of rotation, then the statistics is defined as,

$$U_n = \sum_{i=1}^n \max(\{D_i - 2\pi/n, 0\}) \quad (5)$$

where

$$\begin{aligned} D_i &= \theta_{i+1} - \theta_i, & \text{for } 1 \leq i \leq n-1 \\ D_n &= 2\pi - \theta_n + \theta_1, & \text{for } i=n \end{aligned}$$

If all the circular variables are equally spaced (perfectly uniform) then $U_n = 0$, else $U_n > 0$, which is true for samples of finite size. Large values of U_n indicates clustering of the variables and their distribution non-uniform.

3 Method

In the present work, we have used COMMANDER, SMICA, NILC, SEVEM [62] temperature maps from the latest Planck release and WMAP-ILC [63] temperature map from final WMAP release. As all the above maps correspond to the same CMB realization, any cosmological signal must be consistently detected in all or at least most of them once its origin from any foreground or systematic is ruled out. To usually to improve the signal to noise ratio we convolve a CMB map with some gaussian filter. Though this modifies the $a_{\ell m}$, they do not have any effect on the phases. The map $a_{\ell m}$ for a given ℓ and m can be written as,

$$a_{\ell m} = a_{\ell m}^S + a_{\ell m}^N$$

where $a_{\ell m}^S$ and $a_{\ell m}^N$ represents signal and noise components respectively. The phases of the map corresponding to the ℓ and m can be written as,

$$\psi_{\ell m} = \frac{\mathcal{I}(a_{\ell m}^S) \sin(\psi_{\ell m}^S) + \mathcal{I}(a_{\ell m}^N) \sin(\psi_{\ell m}^N)}{\mathcal{R}(a_{\ell m}^S) \cos(\psi_{\ell m}^S) + \mathcal{R}(a_{\ell m}^N) \cos(\psi_{\ell m}^N)}$$

with \mathcal{R} , \mathcal{I} represents real and imaginary parts, respectively. $\psi_{\ell m}^S$ and $\psi_{\ell m}^N$ are the signals and the noise phase, respectively. From the above phase expression, it is clear that the $\psi_{\ell m}$ will be dominated by signal iff $a_{\ell m}^S \gg a_{\ell m}^N$. For CMB temperature maps, this condition holds for low ℓ , and hence in

order to avoid large contribution to phases from noise, we restrict our analysis to a maximum ℓ mode of 128. We employ `ianafast` facility in `Healpix` [64] package to obtain the spherical harmonic coefficient i.e., $a_{\ell m}$ corresponding to `COMMANDER`, `SMICA`, `NILC`, `SEVEM`, `WMAP` temperature maps. Using the above $a_{\ell m}$ we obtain $\psi_{\ell m}$ applying (4) for ℓ mode 2 to maximum ℓ mode 128 for all the maps. From the above-acquired phases, we investigate for two distinct classes of correlations. In class I we investigate correlations among phases of the same ℓ modes; in class II we investigate correlations between subsequent and next to subsequent ℓ mode phases. For the class I, we used three variable types each indicated by following cases in our analysis, where i is the map index:

Case (i) : $\{\psi_{\ell,m}^i\}$ set of all phases for a given ℓ mode, for testing the uniformity of phases in each mode.

Case (ii) : $\{\psi_{\ell,m+1}^i - \psi_{\ell,m}^i\}$, difference of phases for a given ℓ but consecutive m , to test the correlation between consecutive m modes.

Case (iii) : $\{\psi_{\ell,m+2}^i - \psi_{\ell,m}^i\}$, difference of phases for a given ℓ but next to consecutive m , to test the correlation between next to consecutive m modes.

For the class II, we used two types of variables indicated by following cases in our analysis :

Case (iv) : $\{\psi_{\ell+1,m}^i - \psi_{\ell,m}^i\}$, difference of phases for a given m but consecutive ℓ , to test the correlation between consecutive ℓ modes but same m .

Case (v) : $\{\psi_{\ell+2,m}^i - \psi_{\ell,m}^i\}$, difference of phases for a given m but next to consecutive ℓ , to test the correlation between next to consecutive ℓ modes but same m .

For the cases (ii–v) where the variable is defined as the difference between two uniform variables, we transform the triangular distribution so obtained to the uniform by adding 2π to any value less than zero. We use the Rao statistics (5) to get values of U_n for all of the above five cases and each map. To examine whether the obtained U_n value is anomalous, we compare it against U_n obtained from 10000 Monte Carlo simulated sets of uniform circular variables. We plot p-value versus ℓ modes for all different maps together for each case in Figure 1 to Figure 5 and mark 0.95 and 0.99 p levels to ascertain significant and highly significant correlated occurrences, with 0.05 and 0.01 probability of type I errors respectively.

4 Results

In this section, we summarise all the results we have obtained after utilizing the Rao's statistics on various variable sets, as elaborated in the above sec-

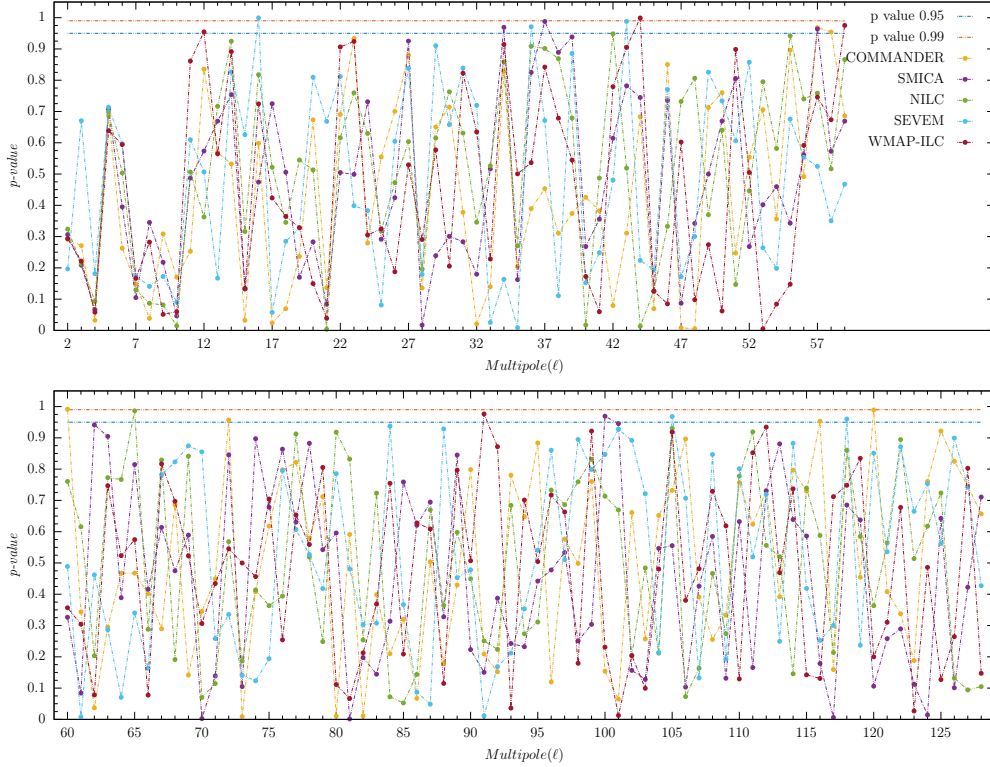


Figure 1: Plot showing p-values of Rao's Statistics for set of phases for various ℓ modes and all maps for the case (i). The two critical levels with $\alpha = 0.05$ (blue dashed line) and $\alpha = 0.01$ (orange dashed line) are also marked to identify significant and highly significant occurrences respectively.

tion, for testing uniformity and correlations. In each of the Figures 1 through 5, the orange and the blue dashed lines represent highly significant ($\alpha = 0.01$) and significant ($\alpha = 0.05$) levels respectively. P-values for all maps and the same variable type are presented together on each of the Figures.

COMM.	SMICA	NILC	SEVEM	WMAP
57(0.9682)			16(0.9991)	12(0.9547)
58(0.9541)	34(0.9690)		36(0.9709)	44(0.9990)
60(0.9916)	37(0.9878)	65(0.9862)	43(0.9880)	59(0.9752)
72(0.9574)	57(0.9638)		105(0.9682)	91(0.9764)
116(0.9532)	100(0.9693)		118(0.9602)	
120(0.9892)				

Table 1: Table showing the significant and high significant occurrences corresponding to Case (i) for various maps.

For the case (i), we tested for uniformity in phases of individual modes, the p-values for all the modes from ℓ mode 2 to 128 are shown in the Figure

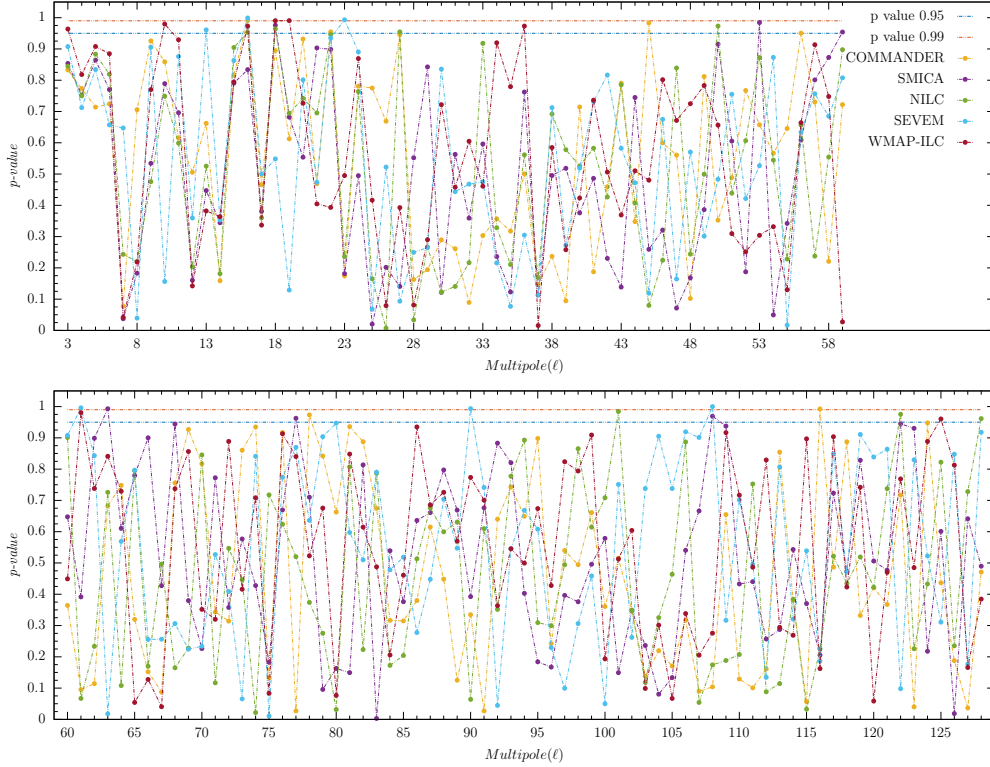


Figure 2: Plot showing p-values of Rao Statistics for constant ℓ mode but difference of consecutive m modes i.e. the case (ii). P-values for all different maps are shown together. The two critical levels with $\alpha = 0.05$ (blue dotted line) and $\alpha = 0.01$ (orange dotted line) are also marked to identify occurrences which are significant and highly significant respectively.

1. Various statistically significant non-uniformity in phases using the Rao's statistics are summarised in Table 1 for COMMANDER(COMM.), SMICA, NILC, SEVEM, and WMAP ILC maps. The first number is shown in all of the Tables 1 to 5 are the significant ℓ mode or representative ℓ mode, corres-

COMM.	SMICA	NILC	SEVEM	WMAP
		16(0.9531)		3(0.9637)
16(0.9905)	18(0.9757)	18(0.9643)	13(0.9609)	10(0.9795)
22(0.9546)	53(0.9843)	27(0.9545)	16(0.9990)	16(0.9731)
45(0.9829)	59(0.9540)	50(0.9733)	23(0.9931)	18(0.9904)
56(0.9503)	63(0.9931)	101(0.9843)	61(0.9958)	19(0.9905)
78(0.9735)	77(0.9625)	122(0.9754)	90(0.9933)	36(0.9730)
116(0.9925)	108(0.9690)	128(0.9616)		61(0.9806)
				125(0.9604)

Table 2: Table showing the significant and high significant occurrences corresponding to Case (ii) for various maps.

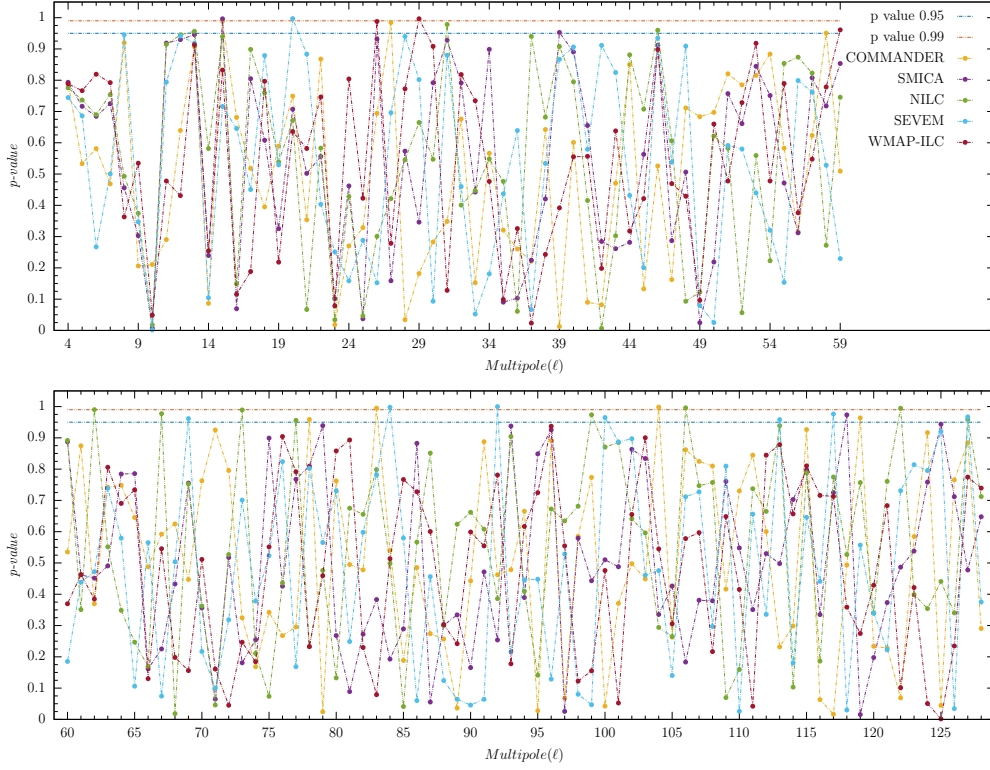


Figure 3: Plot showing p-values of Rao Statistics for constant ℓ mode but difference of next to consecutive m modes i.e. case (iii). P-values for all different maps are shown together. The two critical levels with $\alpha = 0.05$ (blue dotted line) and $\alpha = 0.01$ (orange dotted line) are also marked to identify occurrences which are significant and highly significant respectively.

ponding to which p-values of U is shown in adjoining small bracket. It can

COMM.	SMICA	NILC	SEVEM	WMAP
		13(0.9563)		
		31(0.9783)		
15(0.9889)		46(0.9598)	20(0.9971)	
27(0.9844)		62(0.9901)	69(0.9615)	
58(0.9506)	15(0.9963)	67(0.9773)	84(0.9978)	26(0.9879)
78(0.9589)	39(0.9527)	73(0.9892)	92(0.9998)	29(0.9964)
83(0.9949)	118(0.9734)	77(0.9558)	100(0.9650)	59(0.9609)
104(0.9981)		99(0.9736)	113(0.9583)	
119(0.9638)		106(0.9961)	117(.9763)	
		122(0.9946)	127(0.9669)	
		127(0.9589)		

Table 3: Table showing the significant and high significant occurrences corresponding to Case (iii) for various maps.

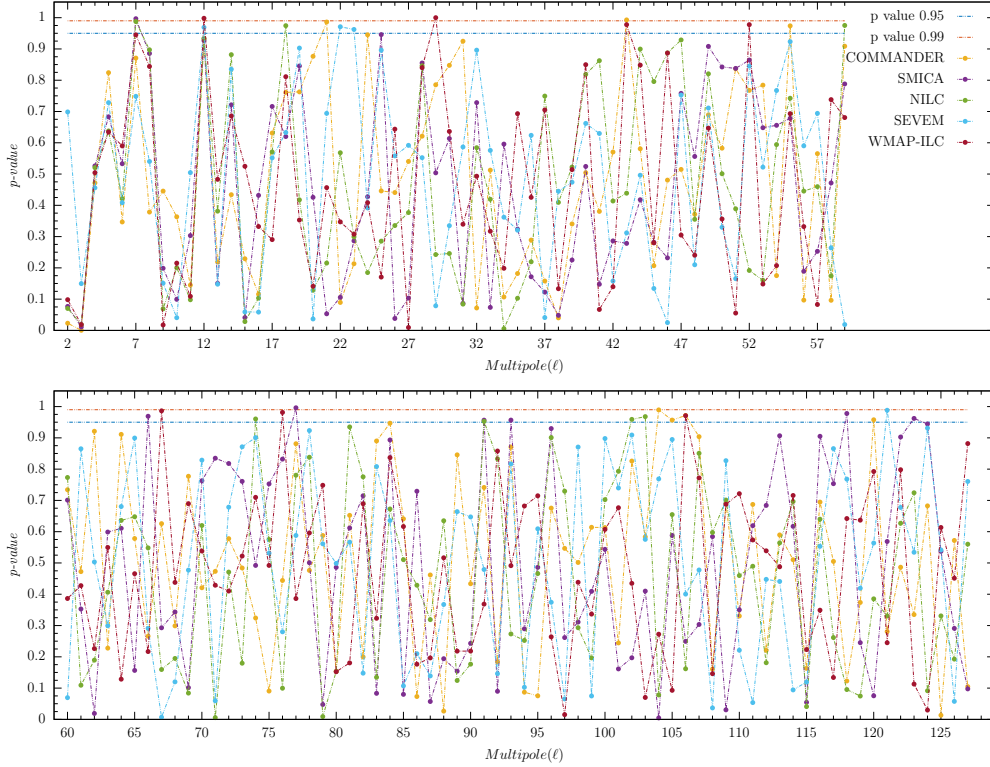


Figure 4: Plot showing p-values of Rao Statistics for difference of phases, for constant m modes but consecutive ℓ modes. The multipole axis represents the lower of the pair of modes involved. Here case (vi) has been plotted for all maps together. The two critical levels with $\alpha = 0.05$ (blue dotted line) and $\alpha = 0.01$ (orange dotted line) are also marked to identify occurrences which are significant and highly significant respectively.

be observed from the Figure 1 that none of the statistically significant occurrences are consistently present in all the maps, with the exception of ℓ mode 57, which is found to be significant in both COMMANDER and SMICA. The phases corresponding to ℓ mode 60 of COMMANDER, 16 of SEVEM, and 44 of WMAP ILC map are of high significance.

COMM.	SMICA	NILC	SEVEM	WMAP
21(0.9860)	7(0.9967)	7(0.9877)		12(0.9980)
43(0.9929)	66(0.9690)	18(0.9743)		29(1.000)
55(0.9738)	77(0.9960)	59(0.9752)	12(0.9690)	43(0.9776)
104(0.9894)	91(0.9565)	74(0.9604)	22(0.9709)	52(0.9776)
105(0.9568)	93(0.9567)	91(0.9529)	23(0.9623)	67(0.9863)
106(0.9716)	118(0.9779)	102(0.9591)	121(0.9883)	76(0.9813)
120(0.9577)	123(0.9622)	103(0.9679)		106(0.9709)

Table 4: Table showing the significant and high significant occurrences corresponding to Case (iv) for various maps.

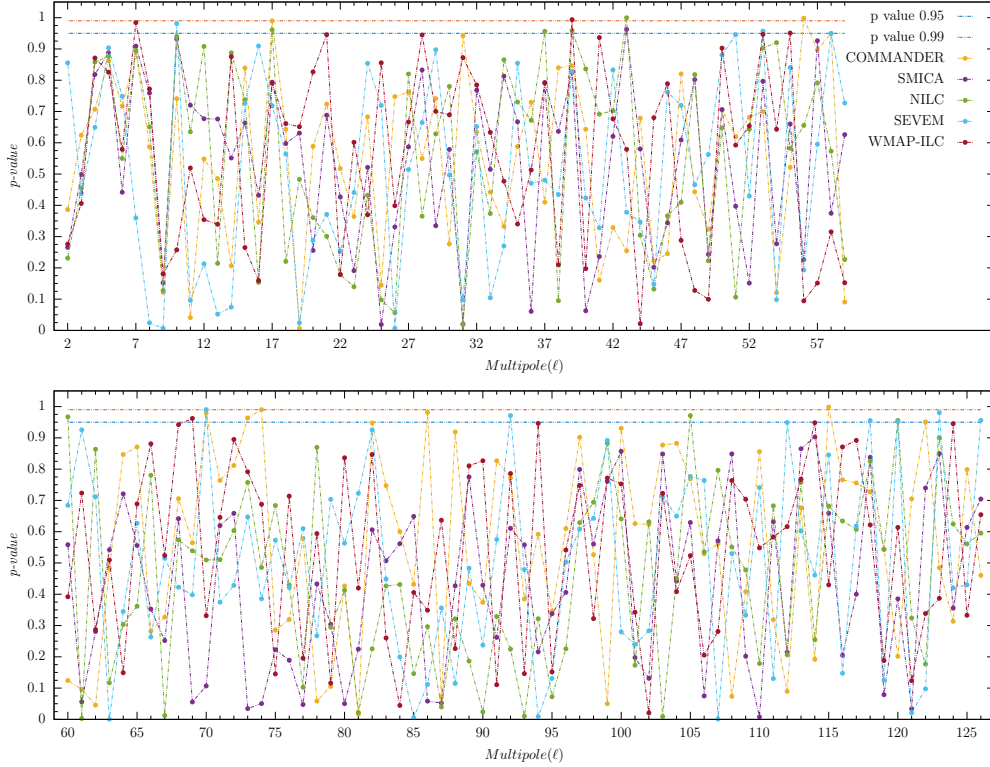


Figure 5: Plot showing p-values of Rao Statistics for difference of phases, for constant m modes but next to consecutive ℓ modes. The multipole axis represents the lower of the pair of modes involved. Case (vii) has been plotted here for all maps together. The two critical levels with $\alpha = 0.05$ (blue dotted line) and $\alpha = 0.01$ (orange dotted line) are also marked to identify occurrences which are significant and highly significant respectively.

COMM.	SMICA	NILC	SEVEM	WMAP
17(0.9898)			10(0.9809)	
56(0.9981)		17(0.9610)	53(0.9571)	
70(0.9793)		37(0.9563)	70(0.9904)	7(0.9841)
73(0.9637)		39(0.9586)	92(0.9711)	39(0.9936)
74(0.9901)	43(0.9625)	43(0.9995)	118(0.9554)	55(0.9508)
86(0.9817)		60(0.9671)	120(0.9517)	69(0.9621)
115(0.9984)		105(0.9712)	122(0.09750)	
122(0.9509)		120(0.9556)	123(0.9806)	
			126(0.9559)	

Table 5: Table showing the significant and high significant occurrences corresponding to Case (v) for various maps.

For the case (ii), we test for correlation among consecutive m mode phases of a given ℓ mode. The Figure 2 for multipole axis starts from $\ell = 3$, as for Rao's statistics, we need at least two variables. The significantly

correlated and highly significant correlated modes are shown in Table 2, along with their respective p-values. For the COMMANDER map the significant modes are 22, 45, 56, 78 and high significant modes are 16 and 116. For the SMICA map 18, 53, 59, 77, 108 are statistically significant modes whereas in mode 63 phase are found to be correlated with high significance. For the NILC map we find correlation within modes 16, 18, 27, 50, 101, 122 and 128 to be statistically significant. For the SEVEM map we found correlation among consecutive m modes significant for phases of ℓ modes 13 and highly significant for 16, 23, 61, 90. For the WMAP consecutive m mode phases of ℓ modes 3, 10, 16, 36, 61, 125 are found to be significantly correlated and m mode phases of ℓ modes 18, 19 are found to be correlated with high significance.

For the case (*iii*), we test for correlation, using U as test statistics, among next to consecutive m mode phase of a given ℓ mode. The plot in Figure 3 on multipole axis starts from $\ell = 4$, for the same reason as mentioned above. We find statistically significant phase correlations between next to consecutive phase in ℓ modes 15, 27, 58, 78, 119 and highly significant correlation in modes 83, 104 for COMMANDER map. We detect high significance correlation in phase of next to consecutive phase in ℓ mode 15 and significant correlation in ℓ mode 39, 118 for SMICA map. For NILC map we find significant correlation in ℓ mode phase

of next to consecutive phase in 13, 31, 46, 67, 73, 77, 99, 127 and high significance correlation in ℓ mode phase 62, 106, 122. For SEVEM map, we find significant detections at 69, 100, 113, 117, 127 ℓ modes and highly significant occurrences at ℓ modes 20, 84, 92. For WMAP we found statistically significant detection at ℓ mode 26, 59 with high significance detection at ℓ mode 59.

For the case (*iv*), we test for correlation using difference of same m mode phases of a ℓ and it's consecutive ℓ mode. The p-values for this analysis are shown in the Figure 4 with the statistically significant cases for all maps shown in Table 4. The multipole axis denotes the lower of the ℓ modes in the pair. We detect significant correlation between same m mode phases of pair (21,22), (55,56), (104,105), (105,106), (106,107), (120,121) with high significance detection in (43,44) for the COMMANDER map. For SMICA map, we find significant correlation between same m mode phases of pair (66,67), (91,92), (93,94), (118,119), (123,124) with high significance in (7,8) and (77,78). For NILC map, we find the pair (7,8), (18,19), (59,60), (74,75), (91,92), (102,103) and (103,104) to be having significant correlation. The pair (12,13), (22,23), (23,24) and (121,122) are the significant occurrences for the SEVEM map. For WMAP ILC map we find pair (29,30), (43,44), (52,53), (67,68), (76,77) and (106,107) significant correlation between same m mode

phases whereas the pair (12,13) is having correlation of high significance.

For the case (v), we do correlation test similar to that of case (iv), but now we take difference of m mode phases in ℓ and next to subsequent ℓ . In Figure 5 with lower of the ℓ in pair represented on the multipole axis, the p-values for various pair are plotted. We find statistically significant detection in pair (17,19), (70,72), (73,75), (86,88), (122,124) and high significance occurrences in (56,58), (74,76), (115,117) for the COMMANDER map. We find only pair (43,45) to be of statistically significant occurrence for the SMICA map. For the NILC map we find significant correlation between same m mode phases of ℓ mode pair (17,19), (37,39), (39,41), (60,62), (105,107), (120,122) with high significance detection in pair (43,45). For the SEVEM map, the statistically significant pair are (10,12), (53,55), (92,94), (118,120), (120,122), (122,124), (123,125), (126,128) with the high significant pair (70,72). For the WMAP, we find the pair (7,9), (55,57), (69,71) to be having statistically significant correlation whereas the pair (39,41) being correlated with high significance.

5 Discussions and Conclusion

In this work we have used Rao's statistic to diagnose potential signatures of non-gaussianity from the observed CMB maps. The CMB component reconstructed maps (COMMANDER, SMICA, NILC, SEVEM, WMAP-ILC) discussed in this work have been obtained by various science groups employing independent statistical techniques by removing foreground emissions. This causes the morphologies and hence phases obtained from these CMB maps to be some what different, although all these CMB maps represent the same last scattering surface. Any significant detection found across different maps is more likely to be of cosmological origin than the ones in a single map, provided the possibility of them being originating from other sources, and unaccounted systematics are ruled out. Not only any detected non-Gaussianities in the CMB temperature maps are essential to understand the distribution of primordial perturbations, but also these detected non-gaussianities have the potentials to constrain residual systematics.

We perform our analysis into three different parts for class I type tests which are designed to detect correlations of phases within a given ℓ mode. The class I type tests consist of three different cases, each of which uses different sets of derived phases. We look for statistically significant multiple occurrences for the same case but different maps, different cases but same map and all cases all maps in class I. With this analysis method, we find that, for the case (i), phases corresponding to most of the modes are uniform, with exceptions for ℓ mode 57 which is occurring multiple times. When considering

high significance cases only, thereby decreasing the probability of type I error, we conclude that the phases corresponding to SMICA, NILC are all uniform. In contrast, some mode phases corresponding to COMMANDER, SEVEM, and WMAP are non-uniform. For the case (ii), phases corresponding to ℓ mode 16 and 18 are significant multiple times across maps, indicating there might be some interesting signal. For the case (iii), phases corresponding to ℓ mode 15 is statistically significant twice across the maps. Looking into the statistical significance across cases (i), (ii), (iii) of the class I for a given map, we find that for the COMMANDER map, ℓ modes 58, 78 and 116 are significant more than one time. Similar repetition of significance for ℓ mode 122 for NILC map, 16 for SEVEM map, and 59 for WMAP are found. We do not find any such repetition for the SMICA map. Considering occurrences of the significance of a ℓ mode across the maps and across the cases for the class I, we conclude that ℓ modes 16, 18, and 59 statistically significant multiple times. To summarise for the class I phases of ℓ mode 15, 16, 18, 57, 58, 59, 78, 116, and 122 have significances occurring multiple times indicating non-gaussianity in corresponding spherical harmonic coefficients which might be of primordial origin.

For the class II tests where we investigate the correlation between neighboring ℓ modes, we look for statistically significant multiple occurrences of correlated pairs. For the class II and case (iv), where we investigate the correlation between subsequent ℓ modes, we find ℓ mode pairs (7,8), (12,13), (43,44), (91,92), and (106,107) occur multiple times with significant correlations across maps. For the class II and case (v), where we investigate the correlation between ℓ and next to subsequent ℓ mode phases, we find that the mode pairs (17,19), (39,41), (43,45), (70,72), (120,122) and (122,124) are significant multiple times across different maps. The presence of non-uniform phases and correlated mode pairs in the cleaned CMB maps establish presence of non-Gaussian signals therein. An important future project will be to investigate the underlying cause of the detected non-gaussianities of this work.

Acknowledgments

SKY acknowledges financial support from Ministry of Human Resource and Development, Government of India via Institute Fellowship at IISER Bhopal, during the course of this work. SKY would like to thank Ujjal Purkayastha for many fruitful discussions during the course of this work. We use the publicly available HEALPix [64] package available to perform spherical harmonic decomposition and for visualization purposes from <http://healpix.sourceforge.net>. We acknowledge the use of the Legacy Archive for Mi-

rowave Background Data Analysis (LAMBDA). LAMBDA is a part of the High Energy Astrophysics Science Archive Center (HEASARC). HEASARC/LAMBDA is supported by the Astrophysics Science Division at the NASA Goddard Space Flight Center. This research has made use of NASA's Astrophysics Data System.

References

- [1] A. H. Guth, *Inflationary universe: A possible solution to the horizon and flatness problems*, *prd* **23** (1981) 347.
- [2] A. D. Linde, *A new inflationary universe scenario: A possible solution of the horizon, flatness, homogeneity, isotropy and primordial monopole problems*, *Physics Letters B* **108** (1982) 389.
- [3] J. M. Bardeen, J. R. Bond, N. Kaiser and A. S. Szalay, *The Statistics of Peaks of Gaussian Random Fields*, *apj* **304** (1986) 15.
- [4] Planck Collaboration, P. A. R. Ade, N. Aghanim, C. Armitage-Caplan, M. Arnaud, M. Ashdown et al., *Planck 2013 results. XXIV. Constraints on primordial non-Gaussianity*, *aap* **571** (2014) A24 [1303.5084].
- [5] Planck Collaboration, Y. Akrami, F. Arroja, M. Ashdown, J. Aumont, C. Baccigalupi et al., *Planck 2018 results. X. Constraints on inflation*, *arXiv e-prints* (2018) arXiv:1807.06211 [1807.06211].
- [6] A. P. S. Yadav and B. D. Wandelt, *Primordial Non-Gaussianity in the Cosmic Microwave Background*, *Advances in Astronomy* **2010** (2010) 565248 [1006.0275].
- [7] J. R. Fergusson, M. Liguori and E. P. S. Shellard, *The CMB bispectrum*, *jcap* **2012** (2012) 032 [1006.1642].
- [8] A. Heavens, M. Santos and P. Ferreira, *The bispectrum of MAXIMA*, *nar* **47** (2003) 815.
- [9] J. Magueijo, *New Non-Gaussian Feature in COBE-DMR 4 Year Maps*, *apjl* **528** (2000) L57 [astro-ph/9911334].
- [10] M. G. Santos, A. Heavens, A. Balbi, J. Borrill, P. G. Ferreira, S. Hanany et al., *Multiple methods for estimating the bispectrum of the cosmic microwave background with application to the MAXIMA data*, *mnras* **341** (2003) 623 [astro-ph/0211123].

- [11] H. B. Sandvik and J. Magueijo, *The complete bispectrum of COBE-DMR four-year maps*, *mnras* **325** (2001) 463 [[astro-ph/0010395](#)].
- [12] P. Cabella, D. Pietrobon, M. Veneziani, A. Balbi, R. Crittenden, G. de Gasperis et al., *Foreground influence on primordial non-Gaussianity estimates: needlet analysis of WMAP 5-year data*, *mnras* **405** (2010) 961 [[0910.4362](#)].
- [13] M. Kunz, A. J. Banday, P. G. Castro, P. G. Ferreira and K. M. Górski, *The Trispectrum of the 4 Year COBE DMR Data*, *apjl* **563** (2001) L99 [[astro-ph/0111250](#)].
- [14] J. R. Fergusson, D. M. Regan and E. P. S. Shellard, *Optimal Trispectrum Estimators and WMAP Constraints*, *arXiv e-prints* (2010) arXiv:1012.6039 [[1012.6039](#)].
- [15] J. Smidt, A. Amblard, A. Cooray, A. Heavens, D. Munshi and P. Serra, *A Measurement of Cubic-Order Primordial Non-Gaussianity (g_{NL} and τ_{NL}) With WMAP 5-Year Data*, *arXiv e-prints* (2010) arXiv:1001.5026 [[1001.5026](#)].
- [16] G. De Troia, P. A. R. Ade, J. J. Bock, J. R. Bond, A. Boscaleri, C. R. Contaldi et al., *The trispectrum of the cosmic microwave background on subdegree angular scales: an analysis of the BOOMERanG data*, *mnras* **343** (2003) 284 [[astro-ph/0301294](#)].
- [17] A. Bernui and M. J. Rebouças, *Searching for non-Gaussianity in the WMAP data*, *prd* **79** (2009) 063528 [[0806.3758](#)].
- [18] A. Bernui and M. J. Rebouças, *Non-Gaussianity in the foreground-reduced CMB maps*, *prd* **81** (2010) 063533 [[0912.0269](#)].
- [19] A. Bernui and M. J. Rebouças, *Mapping possible non-Gaussianity in the Planck maps*, *aap* **573** (2015) A114 [[1405.1128](#)].
- [20] C. R. Contaldi, P. G. Ferreira, J. Magueijo and K. M. Górski, *A Bayesian Estimate of the Skewness of the Cosmic Microwave Background*, *apj* **534** (2000) 25 [[astro-ph/9910138](#)].
- [21] A. Curto, E. Martínez-González and R. B. Barreiro, *Improved Constraints on Primordial Non-Gaussianity for the Wilkinson Microwave Anisotropy Probe 5-Year Data*, *apj* **706** (2009) 399 [[0902.1523](#)].

- [22] A. Curto, E. Martínez-González, P. Mukherjee, R. B. Barreiro, F. K. Hansen, M. Liguori et al., *Wilkinson Microwave Anisotropy Probe 5-yr constraints on f_{nl} with wavelets*, *mnras* **393** (2009) 615 [[0807.0231](#)].
- [23] A. Curto, E. Martínez-González and R. B. Barreiro, *The effect of the linear term on the wavelet estimator of primordial non-Gaussianity*, *mnras* **426** (2012) 1361 [[1111.3390](#)].
- [24] A. Curto, E. Martínez-González, R. B. Barreiro and M. P. Hobson, *Constraints on general primordial non-Gaussianity using wavelets for the Wilkinson Microwave Anisotropy Probe 7-year data*, *mnras* **417** (2011) 488 [[1105.6106](#)].
- [25] P. Mukherjee and Y. Wang, *Wavelets and Wilkinson Microwave Anisotropy Probe Non-Gaussianity*, *apj* **613** (2004) 51 [[astro-ph/0402602](#)].
- [26] P. Cabella, M. Liguori, F. K. Hansen, D. Marinucci, S. Matarrese, L. Moscardini et al., *Primordial non-Gaussianity: local curvature method and statistical significance of constraints on f_{NL} from WMAP data*, *mnras* **358** (2005) 684 [[astro-ph/0406026](#)].
- [27] J. D. McEwen, M. P. Hobson, A. N. Lasenby and D. J. Mortlock, *A high-significance detection of non-Gaussianity in the Wilkinson Microwave Anisotropy Probe 1-yr data using directional spherical wavelets*, *mnras* **359** (2005) 1583 [[astro-ph/0406604](#)].
- [28] X. Liu and S. N. Zhang, *Non-Gaussianity Due to Possible Residual Foreground Signals in Wilkinson Microwave Anisotropy Probe First-Year Data Using Spherical Wavelet Approaches*, *apj* **633** (2005) 542 [[astro-ph/0504589](#)].
- [29] J. D. McEwen, M. P. Hobson, A. N. Lasenby and D. J. Mortlock, *Non-Gaussianity detections in the Bianchi VII_h corrected WMAP one-year data made with directional spherical wavelets*, *mnras* **369** (2006) 1858 [[astro-ph/0510349](#)].
- [30] J. D. McEwen, M. P. Hobson, A. N. Lasenby and D. J. Mortlock, *A high-significance detection of non-Gaussianity in the WMAP 3-yr data using directional spherical wavelets*, *mnras* **371** (2006) L50 [[astro-ph/0604305](#)].
- [31] P. Vielva, E. Martínez-González, R. B. Barreiro, J. L. Sanz and L. Cayón, *Detection of Non-Gaussianity in the Wilkinson Microwave*

- Anisotropy Probe First-Year Data Using Spherical Wavelets*, *apj* **609** (2004) 22 [[astro-ph/0310273](#)].
- [32] M. Cruz, E. Martínez-González, P. Vielva and L. Cayón, *Detection of a non-Gaussian spot in WMAP*, *mnras* **356** (2005) 29 [[astro-ph/0405341](#)].
- [33] R. B. Barreiro, M. P. Hobson, A. N. Lasenby, A. J. Banday, K. M. Górski and G. Hinshaw, *Testing the Gaussianity of the COBE DMR data with spherical wavelets*, *mnras* **318** (2000) 475 [[astro-ph/0004202](#)].
- [34] T. Buchert, M. J. France and F. Steiner, *Model-independent analyses of non-Gaussianity in Planck CMB maps using Minkowski functionals*, *Classical and Quantum Gravity* **34** (2017) 094002 [[1701.03347](#)].
- [35] C. P. Novaes, A. Bernui, G. A. Marques and I. S. Ferreira, *Local analyses of Planck maps with Minkowski functionals*, *mnras* **461** (2016) 1363 [[1606.04075](#)].
- [36] J. H. P. Wu, A. Balbi, J. Borrill, P. G. Ferreira, S. Hanany, A. H. Jaffe et al., *Tests for Gaussianity of the MAXIMA-1 Cosmic Microwave Background Map*, *prl* **87** (2001) 251303 [[astro-ph/0104248](#)].
- [37] G. Polenta, P. A. R. Ade, J. J. Bock, J. R. Bond, J. Borrill, A. Boscaleri et al., *Search for Non-Gaussian Signals in the BOOMERANG Maps: Pixel-Space Analysis*, *apjl* **572** (2002) L27 [[astro-ph/0201133](#)].
- [38] E. Komatsu, *Wilkinson Microwave Anisotropy Probe constraints on non-Gaussianity*, *nar* **47** (2003) 797.
- [39] G. Rossmannith, C. Räth, A. J. Banday and G. Morfill, *Non-Gaussian signatures in the five-year WMAP data as identified with isotropic scaling indices*, *mnras* **399** (2009) 1921 [[0905.2854](#)].
- [40] G. Rossmannith, H. Modest, C. Räth, A. J. Banday, K. M. Górski and G. Morfill, *Search for Non-Gaussianities in the WMAP Data with the Scaling Index Method*, *Advances in Astronomy* **2011** (2011) 174873 [[1108.0596](#)].
- [41] P. Vielva and J. L. Sanz, *Analysis of non-Gaussian cosmic microwave background maps based on the N-pdf. Application to Wilkinson Microwave Anisotropy Probe data*, *mnras* **397** (2009) 837 [[0812.1756](#)].

- [42] Z. Hou, A. J. Banday, K. M. Górski, F. Elsner and B. D. Wandelt, *The primordial non-Gaussianity of local type (f^{local}_{NL}) in the WMAP 5-year data: the length distribution of CMB skeleton*, *mnras* **407** (2010) 2141 [[1005.5568](#)].
- [43] H. K. Eriksen, D. I. Novikov, P. B. Lilje, A. J. Banday and K. M. Górski, *Testing for Non-Gaussianity in the Wilkinson Microwave Anisotropy Probe Data: Minkowski Functionals and the Length of the Skeleton*, *apj* **612** (2004) 64 [[astro-ph/0401276](#)].
- [44] A. Ravenni, M. Liguori, N. Bartolo and M. Shiraishi, *Primordial non-Gaussianity with μ -type and y -type spectral distortions: exploiting Cosmic Microwave Background polarization and dealing with secondary sources*, *jcap* **2017** (2017) 042 [[1707.04759](#)].
- [45] C. P. Novaes, A. Bernui, I. S. Ferreira and C. A. Wuensche, *A neural-network based estimator to search for primordial non-Gaussianity in Planck CMB maps*, *jcap* **2015** (2015) 064 [[1409.3876](#)].
- [46] C. J. Copi, D. Huterer and G. D. Starkman, *Multipole vectors: A new representation of the CMB sky and evidence for statistical anisotropy or non-Gaussianity at $2 \leq l \leq 8$* , *prd* **70** (2004) 043515 [[astro-ph/0310511](#)].
- [47] C.-G. Park, *Non-Gaussian signatures in the temperature fluctuation observed by the Wilkinson Microwave Anisotropy Probe*, *mnras* **349** (2004) 313 [[astro-ph/0307469](#)].
- [48] C.-G. Park, C. Park, B. Ratra and M. Tegmark, *Gaussianity of Degree-Scale Cosmic Microwave Background Anisotropy Observations*, *apj* **556** (2001) 582 [[astro-ph/0102406](#)].
- [49] L. G. Book, M. Kamionkowski and T. Souradeep, *Odd-parity bipolar spherical harmonics*, *prd* **85** (2012) 023010 [[1109.2910](#)].
- [50] P. Coles, P. Dineen, J. Earl and D. Wright, *Phase correlations in cosmic microwave background temperature maps*, *mnras* **350** (2004) 989 [[astro-ph/0310252](#)].
- [51] L.-Y. Chiang and P. D. Naselsky, *Phase and Cross-Correlation of Phases of the Whole-Sky CMB and Foreground Maps from the 1-YEAR Wmap Data*, *International Journal of Modern Physics D* **15** (2006) 1283 [[astro-ph/0407395](#)].

- [52] A. Kovács, I. Szapudi and Z. Frei, *Phase statistics of the WMAP 7 year data*, *Astronomische Nachrichten* **334** (2013) 1020 [[1308.0837](#)].
- [53] D. L. Larson and B. D. Wandelt, *A Statistically Robust 3-Sigma Detection of Non-Gaussianity in the WMAP Data Using Hot and Cold Spots*, *arXiv e-prints* (2005) astro [[astro-ph/0505046](#)].
- [54] L.-Y. Chiang, P. D. Naselsky, O. V. Verkhodanov and M. J. Way, *Non-Gaussianity of the Derived Maps from the First-Year Wilkinson Microwave Anisotropy Probe Data*, *apjl* **590** (2003) L65 [[astro-ph/0303643](#)].
- [55] L.-Y. Chiang, P. D. Naselsky and P. Coles, *The Robustness of Phase Mapping as a Non-Gaussianity Test*, *apjl* **602** (2004) L1 [[astro-ph/0208235](#)].
- [56] P. D. Naselsky, A. G. Doroshkevich and O. V. Verkhodanov, *Cross-correlation of the phases of the CMB and foregrounds derived from the WMAP data*, *mnras* **349** (2004) 695 [[astro-ph/0310601](#)].
- [57] P. Naselsky, L.-Y. Chiang, P. Olesen and I. Novikov, *Statistics of phase correlations as a test for non-Gaussianity of the CMB maps*, *prd* **72** (2005) 063512 [[astro-ph/0505011](#)].
- [58] B. D. Wandelt, *Statistical Challenges of Cosmic Microwave Background Analysis*, *arXiv e-prints* (2004) astro [[astro-ph/0401622](#)].
- [59] Jammalamadaka S.Rao, and Sengupta, Ambar, *Topics in Circular Statistics*, vol. 5 of *Series On Multivariate Analysis*, ch. Nonparametric Testing Procedures, pp. 161–164. World Scientific, FIRST ed., 2001.
- [60] J. S. Rao, *Some tests based on arc-lengths for the circle*, *Sankhya: The Indian Journal of Statistics, Series B (1960-2002)* **38** (1976) 329.
- [61] N. H. Kuiper, *Tests concerning random points on a circle.*, *Proc. Koninkl. Nederl. Akad. Van Wetenschappen, Series A* (1960) 38.
- [62] Planck Collaboration, Y. Akrami, M. Ashdown, J. Aumont, C. Baccigalupi, M. Ballardini et al., *Planck 2018 results. IV. Diffuse component separation*, *arXiv e-prints* (2018) arXiv:1807.06208 [[1807.06208](#)].
- [63] C. L. Bennett, D. Larson, J. L. Weiland, N. Jarosik, G. Hinshaw, N. Odegard et al., *Nine-year Wilkinson Microwave Anisotropy Probe*

(WMAP) *Observations: Final Maps and Results*, *apjs* **208** (2013) 20 [1212.5225].

- [64] K. M. Górski, E. Hivon, A. J. Banday, B. D. Wandelt, F. K. Hansen, M. Reinecke et al., *HEALPix: A Framework for High-Resolution Discretization and Fast Analysis of Data Distributed on the Sphere*, *apj* **622** (2005) 759 [arXiv:astro-ph/0409513].